Jurnal Teknik Mesin
Mechanical Xplore (JTMMX)
Mechanical Engineering
Vol. 5 No. 2 (2024) pp. 051-068
p-ISSN: 2746-0045 e-ISSN: 2746-3672

Unraveling the Potential of Coconut Shell Activated Carbon for Catalytic Converter Application: A Preliminary Studies of its Optimization through the Assisted of Fuzzy Logic

Diansyah Marbun[1], Muhamad Taufik Ulhakim[1*], Sukarman Sukarman[1], Agus Supriyanto[1], Ade Suhara[2], Auliya Rahmatul Ummah[3], Neng Astri Lidiawati[4]

[1]Department of Mechanical Engineering, Faculty of Engineering, Universitas Buana Perjuangan Karawang, Karawang, 41361, West Java, Indonesia
[2]Department of Industrial Engineering, Faculty of Engineering, Universitas Buana Perjuangan Karawang, Karawang, 41361, West Java, Indonesia
[3]Department of Physics, Faculty of Mathematic and Natural Sciences, Universitas Mulawarman, Samarinda, 75119, East Kalimantan, Indonesia
[4]Department of Engineering Physics, Faculty of Industrial Technology, Institut Teknologi Bandung, Bandung, 40132, West Java, Indonesia

ABSTRACT

Nowadays, researchers focus on developing catalytic converters based on activated carbon (AC) from organic waste to address environmental concerns. This study presents a preliminary investigation into the application of catalytic converters through the synthesis of AC from coconut shells, with optimization achieved through the implementation of fuzzy logic to ascertain the optimal properties of the AC, specifically the activation temperature. The fuzzy logic approach has determined that the optimal activation temperature is 950 °C. The effectiveness of this approach is substantiated by the successful synthesis of AC, as evidenced by XRD, FTIR, and SEM-EDX analysis. The findings indicate that fuzzy logic provides the most accurate activation temperature information, significantly impacting the AC structure. The resulting yield and bulk density values were 26.29% and 0.519 g/ml, respectively. Proximate analysis indicates that the ash content (4.332%), moisture (7.211%), and volatile matter (16.321%) achieve an FCC of 72.136%. The iodine number is a crucial parameter in evaluating the potential application of AC for the catalytic converter. The results demonstrated that the adsorption performance is achieved in 613 mg/g. In conclusion, the AC produced shows considerable potential for use as a catalytic converter. This assertion is substantiated by the successful evaluation of its efficacy in reducing CO and HC, respectively, by approximately 86.04% and 56.79%. To confirm the suitability of the catalytic converter for the vehicle. A series of dynamometer tests were conducted to verify the catalytic converter's performance. The ensuing test results exhibited a decline in torque and power values; however, these measurements remained within acceptable parameters for typical daily utilization.

Keywords: Coconut shell, Activated carbon, Fuzzy logic, Catalytic converter, Dynamometer tests.

Article information:
Submitted: 28/01/2025
Revised: 30/01/2025
Accepted: 01/02/2025
Published: 15/02/2025

Author correspondence:
* ✉: muhamad.ulhakim@ubpkarawang.ac.id

Type of article:

☑ Research papers

☐ Review papers

1. Introduction

Despite the fact that gasoline motors have been meticulously crafted and utilize cutting-edge technology, a number of studies have indicated that gasoline motors are a significant contributor to pollution in urban environments. These engines emit a range of toxic gases, including hydrocarbons (HC), carbon monoxide (CO), and nitrogen oxides (NOx) [1]. The automotive industry has been a signifi-

cant contributor to air pollution, accounting for approximately 27% of emissions. Consequently, reducing carbon output in this sector is crucial for attaining global climate stability [2]. To achieve this objective, several regulations have been established regarding exhaust emission standards for vehicles. These include the Euro VI standard, the Environmental Protection Agency (EPA) standard in the United States, and the China VI-b standard [3]. It is, of course, the intention that all vehicles produced must comply with the relevant exhaust gas standards in their respective regions. Furthermore, to comply with pertinent regulations, approximately 85% of vehicles currently in production are equipped with catalytic converters [4].

A catalytic converter is a critical vehicle component designed to transform toxic exhaust emissions into environmentally friendly gases [5]. Various types of catalytic converters exist, including oxidation catalysts [6], particulate filter catalytic converters [7], lean NOx trap (LNT) catalysts [8], selective catalytic reduction (SCR) catalysts [9], and three-way catalytic converters (TWC) [10]. Among these, TWC demonstrates the highest potential under specific operating conditions [11] as it simultaneously reduces hydrocarbon (HC), carbon monoxide (CO), and nitrogen oxide (NOx) emissions in internal combustion engines, offering a competitive advantage [12]. Gunasekaran *et al.* [13] reported that TWC can effectively reduce HC, CO, and NOx emissions by 55%, 38%, and 45%, respectively, while other studies have indicated reductions of 60% for HC and CO, and up to 70% for NOx [14]. Despite its effectiveness, the TWC has notable drawbacks, including a stoichiometric operation requirement that compromises the engine efficiency. Additionally, the cost of certain TWC components poses a financial challenge [15-16].

Given these limitations, researchers have explored alternative catalytic converter technologies based on activated carbon (AC) [17-21]. AC's porous structure and high surface area of AC make it an excellent adsorbent material [22]. Hamid *et al.* [23] demonstrated that AC derived from banana peels could reduce CO and NOx emissions by approximately 57% and 43%, respectively. Similarly, Fajri and Ghofur [24] found that the AC from ulin wood reduced CO and HC emissions by 52.23% and 85.63%, respectively. Sulton and Ghofur [25] further confirmed the effectiveness of AC from alaban wood, achieving reductions of 75.69% for CO and 81.67% for HC emissions. These studies highlight the potential of AC-based catalytic converters, particularly doughnut-shaped configurations, which enhance exhaust gas flow and prevent congestion.

AC can be synthesized from agricultural waste, with coconut shell (CS) emerging as a promising precursor due to its high carbon content and favorable physicochemical properties [26]. AC derived from CS is distinguished by its high carbon content and favorable inherent properties [27]. However, the structural characteristics of AC are highly dependent on synthesis parameters such as heating rate, activation time, chemical agents, and activation temperature [28-29]. Among these, the activation temperature plays a critical role in determining the pore structure and adsorption capacity of AC [30]. The optimal activation temperature typically ranges from 900 to 1000 °C [31], but precise optimization within this range is required. Therefore, this study aimed to evaluate the influence of activation temperature on the structural and catalytic properties of AC derived from CS to ensure its suitability for emission control applications.

Recent studies have explored various approaches to optimize material synthesis parameters, particularly for the production of activated carbon (AC). Rajkumar *et al.* [32] demonstrated that fuzzy logic is an effective tool for optimizing synthesis conditions, providing a systematic framework for identifying the most suitable parameters. Similarly, Wang *et al.* (2023) highlighted the advantages of fuzzy logic in accelerating the optimization process, reducing the computational time, and enhancing the overall process efficiency [33]. Given these benefits, fuzzy logic has been widely adopted for parameter optimization in material-processing applications. In this study, fuzzy logic was employed to determine the optimal activation temperature for AC derived from CS to enhance its physicochemical properties and overall performance.

This study presents an initial investigation into the fabrication of AC-based catalytic converters. This study focuses on examining the characteristics of AC derived from CS that has been optimized at an activation temperature using fuzzy logic. The characteristics include physical properties, proximate analysis, and adsorption performance based on the iodine number. Furthermore, this study conducted direct testing related to the benefits of the AC in reducing exhaust emissions. AC is formed into a catalytic converter and is applied to vehicles. Furthermore, this study encompassed the execution of additional evaluative procedures, including power and torque assessments using dynamometer testing. This evaluation was conducted to assess the performance of the vehicle both prior to and following the implementation of the catalytic converter. Additionally, this evaluation was undertaken to ascertain the impact of incorporating an activated carbon-based catalytic converter on vehicle engine performance. These preliminary tests were conducted as a prelude to the subsequent large-scale production of AC, which is intended for application as an advanced catalytic converter in the future. The operational principle of the catalytic converter based on AC depends on its capacity to absorb the toxic gases produced by vehicles. The authors posit that this research will prove instrumental in identifying AC with optimal properties, which will have a significant impact on technological advancement. As a catalytic converter, it facilitates the reduction of air pollution, thereby enabling the creation of environmentally friendly vehicles.

2. Methods

2.1. Fuzzy logic methodology

Fuzzy logic was used to determine the best activation temperature for AC. Previous studies [31] have demonstrated that AC exhibits optimal activation at temperatures ranging from 900 to 1000 °C. The values were processed using fuzzy logic to determine the optimal activation temperature. As illustrated in Figure 1, the fuzzy logic process comprises multiple steps. Fuzzy logic is chosen because it is the most powerful technique for determining the relationship between the input and output. With this approach, fuzzy logic manages uncertainty and process variability, providing optimal results despite the ambiguous nature of inputs. This system is effective in improving the efficiency and quality of AC [34].

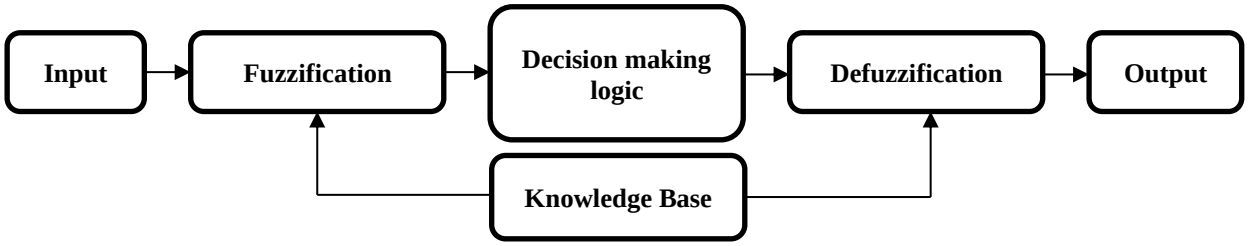

Figure 1. Fuzzy logic system.

The initial step in the process entails the transformation of temperatures into fuzzy values through the utilization of membership functions, such as “low”, “medium”, and “high” [35]. For instance, a temperature of 900°C could be classified as "low," whereas a temperature of 1000°C could be designated as “high.” This temperature was maintained for a predetermined duration of one hour during the activation procedure. The process of converting crisp-valued data into fuzzy data is referred to as fuzzification, also known as membership function [36]. Equation 1 illustrates the implementation of the triangular membership function in this study.

$$\mu_{\text{triangular}}(x) = \begin{cases} 0, & \text{if } x \le a \\ \frac{x-a}{b-a}, & \text{if } a \le x \le b \\ \frac{c-x}{c-b}, & \text{if } b < x \le b \\ 0, & \text{otherwise} \end{cases} \quad (1)$$

The selection of triangular membership functions is driven by their numerous advantages, including straightforward interpretation, ease of use, and intuitive representation [37]. The triangular membership function offers flexibility and efficiency, rendering it particularly well suited for scenarios in which the effective temperature range (e.g., 900–1000 °C) can be delineated with a lower limit, an optimal temperature, and an upper limit. In the context of AC synthesis, the use of a triangular membership function ensures that the system operates at the optimal temperature, thereby yielding optimal outcomes. This is achieved by considering the chemical and physical characteristics that affect the activation process.

A knowledge base comprising "If-Then" rules is employed, such as "if the temperature is low, then the carbon quality is low" or "if the temperature is high, then the carbon quality is optimal." The decision-making logic processes these rules using fuzzy operations, such as AND and OR, to produce fuzzy outputs. The fuzzy results were then converted to crisp values through defuzzification. For example, the centroid method is used. The final output is an optimal temperature recommendation that can be used to set the activation temperature [38].

2.2. Chemicals and Instrumentations

The primary raw material used in this study was CS, which was collected from Karawang, West Java. Chemical activation was performed using phosphoric acid (H_3PO_4) and deionized water to enhance the porosity of the carbonized materials. Microporosity characterization was conducted through iodine number analysis, which required hydrochloric acid (HCl), sodium thiosulfate ($Na_2S_2O_3$), and starch. All chemicals were purchased from Merck and used as received.

The instrumentation utilized in this study included a muffle furnace (Naberthem) for carbonization, along with a crucible and lid for sample containment. A 200-mesh sieve filter was used to ensure a uniform particle size distribution. Proximate analysis of the activated carbon was conducted to determine the ash content, moisture content, volatile matter, and fixed carbon content (FCC). Further structural, chemical, and morphological characterizations were carried out using X-ray diffraction (XRD) with a MiniFlex Benchtop Diffractometer, Fourier-transform infrared (FTIR) spectroscopy using a Bruker Alpha II, and scanning electron microscopy-energy dispersive X-ray (SEM-EDX) with a Hitachi TM SU-3500.

Copper (Cu) powder and polyvinyl alcohol (PVA) were used as binding agents for the catalytic converter. The activation process was conducted at various temperatures and durations to optimize the physicochemical properties of the activated carbon. The final samples were comprehensively characterized to assess their structural integrity, surface chemistry, and morphological features. These analyses provide crucial insights into the properties and performance of CS-derived activated carbon, particularly for its application in catalytic converter fabrication.

2.3. Preparation of activated carbon materials

Activated carbon (AC) was synthesized from CS through a chemical activation process using phosphoric acid (H_3PO_4) as the activating agent, as illustrated in Figure 2. Initially, the CS was crushed into small pieces and thoroughly washed with deionized water to remove any impurities. The cleaned material was then subjected to solar drying for approximately three days, followed by oven drying at 110 °C for 5 h to eliminate any residual moisture. After drying, the CS was ground into a fine powder and sieved using a 200-mesh filter to ensure a uniform particle size distribution.

The sieved material was immersed in 50 mL of phosphoric acid solution and stirred at 600 rpm for 1 h to facilitate chemical treatment. Subsequently, the impregnated material was filtered and dried at 100 °C for 5 h. The dried sample was then subjected to an activation process at a temperature determined by fuzzy logic analysis, with an estimated processing time of 1 h. This optimized activation step aimed to enhance the physicochemical properties of the resulting activated carbon.

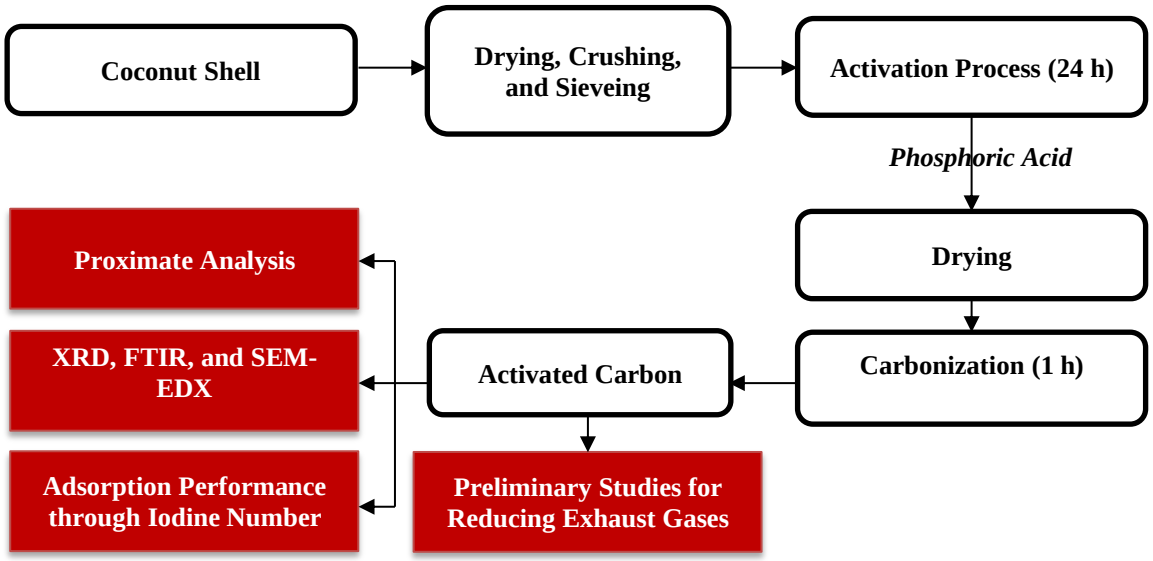

Figure 2. Activated carbon preparation process from CS.

2.4. Characterization and physical properties

The structural, chemical, and morphological properties of AC were analyzed using XRD, FTIR, and SEM-EDX. XRD analysis was conducted to determine the crystallinity or amorphous nature of the synthesized AC, employing Cu-Kα radiation (λ = 0.15406 Å) over a diffraction angle range of 10°–80°. FTIR spectroscopy was utilized to identify surface functional groups within the AC, with spectral data collected in the mid-infrared region (4000–500 cm^{-1}), following the methodology described in previous studies [40]. SEM-EDX analysis was performed to determine the elemental composition of the AC and to assess the effectiveness of the synthesis process [41].

In addition to structural characterization, the physical properties of AC were evaluated through yield and bulk density measurements. The AC yield was calculated using Equation 2, defined as the ratio of the final AC weight to the initial weight of raw coconut shell, expressed as a percentage [42]. Bulk density was determined using Equation 3, adapted from Muleta (2024) [43], with slight modifications. The AC sample was weighed and placed in a graduated cylinder, followed by the addition of liquid until the sample was fully submerged. The total volume of the cylinder, including the AC, was then recorded to determine the bulk density. These analyses provide insights into the physicochemical properties of AC and its suitability for further applications.

$$\text{Yield (\%)} = \frac{\text{Weight of activated carbon (g)}}{\text{Weight of raw material (g)}} \text{x } 100\% \quad (2)$$

$$\text{Bulk density} = \frac{\text{mass of activated carbon (g)}}{\text{volume of sample in the cylinder (ml)}} \quad (3)$$

2.5. Fixed carbon content

Proximate analysis was conducted to determine the fixed carbon content (FCC), along with ash content, moisture content, and volatile matter. These analyses were performed in accordance with ASTM standards, specifically ASTM D2866 [44] for ash conten, D2867 [45] for moisture content, and D5832 [46] for volatile matter determination.. The FCC was calculated using Equation 4 [47], providing insight into the carbonization efficiency and quality of the produced activated carbon.

$$\text{FCC (\%)} = 100\% - (\%A + \%M + \%V) \quad (4)$$

where %A, %M, and %V indicate the percentages of ash, moisture, and volatile matter, respectively. Accordingly, to calculate the FCC, it is necessary to obtain the aforementioned values.

To determine the ash content, 1 g of AC was placed into a crucible and heated to 650 °C for approximately 3 h. Thereafter, the remaining AC was weighed, and the ash content was calculated using Equation 5 [48]. The moisture content was then determined using a series of steps. Initially, the crucible was weighed, and then 1 g of AC was placed into the crucible. The weight is recorded. The crucible was then heated at 150 °C for approximately 2 h and cooled to room temperature. Subsequently, the crucible with the AC inside was weighed again, and the moisture content was calculated using Equation 6 [49], where m_0 represents the weight of the crucible, m_1 signifies the weight of the crucible with the AC inside prior to the heating treatment, and m_2 denotes the weight of the crucible with the AC inside following the heating treatment.

$$\text{Ash (\%)} = \frac{\text{Weight of remaining activated carbon (g)}}{\text{Initial weight of the activated carbon prior to heating (g)}} \text{ x } 100\% \quad (5)$$

$$\text{Moisture (\%)} = \frac{m_1 - m_2}{m_1 - m_0} \text{ x } 100\% \quad (6)$$

The procedure for determining the volatile matter, as described by Fito in 2023 [50], was as follows: 1 g of AC was heated at 950 °C for ~ 10 min. The sample was then cooled to room temperature. Subsequently, the sample was weighed to observe the change in weight resulting from the heating treatment. The volatile matter was calculated using Equation 7.

$$\text{Volatile (\%)} = \frac{A - B}{C - B} \text{ x } 100\% \quad (7)$$

Where A weight of the sample after the heating treatment, C is the weight of the sample before the heating treatment, and B is the weight of the crucible used during this phase.

2.6. Iodine number determination

The iodine number was analyzed according to ASTM D4607 [51]. The iodine number was determined through a series of steps, beginning with weighing 1 g of AC. The sample was then transferred to an Erlenmeyer flask containing 10 ml of 5% hydrochloric acid and boiled for approximately 30 s. The solution was then cooled to room temperature. An iodine solution with a concentration of 0.1 M and volume of 100 ml was introduced. The solution was then agitated for approximately 30 s. The mixture was filtered, and the filtrate was set aside for further analysis. The remaining 50 ml of filtrate was titrated with 0.1 M sodium thiosulfate until the solution exhibited a light yellow coloration. The solution was then titrated with starch as an indicator until it displayed a blue coloration, which was repeated until a colorless solution was achieved. The iodine number is employed as a means of observing the extent of microporosity present in AC [52]. The quantity of iodine adsorbed per gram of AC was determined using Equation 8 [53]. The microporosity of AC is a crucial factor in determining its efficacy for the adsorption of small molecules. A higher iodine number indicates a greater degree of microporosity in the AC [54-55]. For catalytic converter applications, the high microporosity of AC represents a significant advantage, given that the fundamental operational principle of AC-based catalytic converters is the adsorption of noxious molecules present in motor vehicle exhaust gases, thereby rendering the resulting exhaust gases more environmentally friendly [20].

$$Iodine\ Number = \frac{[(N_1 * 12693) - (2.2 * N_1 * 126.93 * S)]}{M} \quad (8)$$

Where, N_1 represents the normality of the iodine solution (N), N_2 denotes the normality of the sodium thiosulfate solution (N), S refers to the volume of sodium thiosulfate (mL), and M indicates the mass of activated carbon (g).

2.7. Fabrication of an Activated Carbon-Based Catalytic Converter

The AC-based catalytic converter was constructed using a doughnut-shaped model, with specifications and measurements presented in Figure 3(a). The manufacturing process necessitated the incorporation of supplementary materials, such as Cu powder and PVA. Cu powder is essential for maintaining the stability of the catalytic converter and exhibits high thermal conductivity [56], whereas PVA functions as a binding agent, to enhance the structural integrity of the catalytic converter [57].The AC-based catalytic converter was fabricated by combining AC, Cu powder, and PVA in an 80%:15%:5% (16:3:1) ratio. Figure 3(b) shows the mold of the manufactured catalytic converter. To evaluate the efficacy of AC-based catalytic converters in reducing vehicle exhaust emissions, direct testing was conducted. This assessment involved positioning the catalytic converter within the vehicle exhaust system, as shown in Figure 3(c). Gas analyzer instruments were used to measure the performance. This initial investigation examined AC's potential of AC as a catalytic converter by focusing on CO and HC emission analyses. Furthermore, vehicles equipped with catalytic converters are subjected to dynamometer testing to determine their performance. In this instance, the assessment concentrates on the engine output, specifically whether there has been a significant decrease in performance. If the engine does not exhibit such a reduction, the catalytic converter can be implemented in motor vehicles and subjected to further evaluation on an industrial scale.

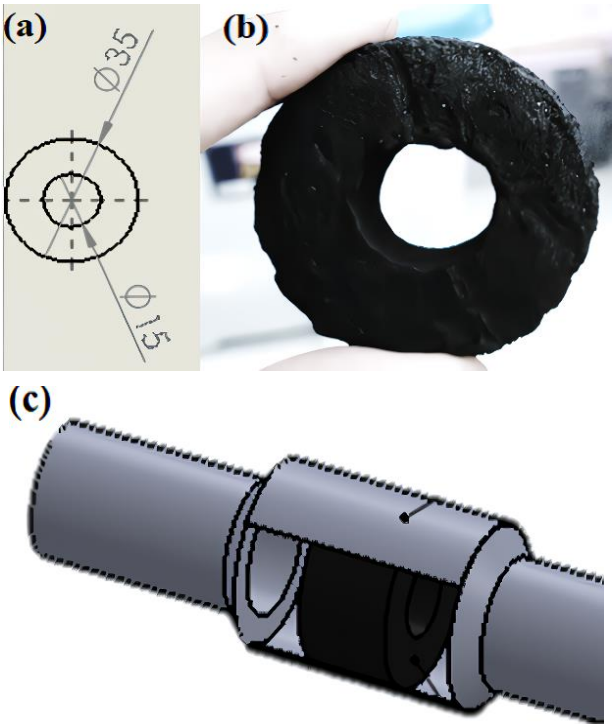

Figure 3. Fabrication of the AC: (a) Design and dimensions of the catalytic converter, (b) catalytic converter based on activated carbon fabricated in this work, and (c) illustration of the catalytic converter in the exhaust.

3. RESULT AND DISCUSSIONS

3.1. Fuzzy logic and proximate analysis

Fuzzy logic serves as an effective methodology for determining the optimal conditions for AC synthesis. A critical component of this approach is the triangular membership function, which is employed to identify the optimal activation temperature. **Figure 4** illustrates the findings of this study. The results indicate that 950 °C (medium-membership function) is the most suitable activation temperature for producing high-quality AC. This finding corresponds to the optimization membership function, which exhibits a membership degree of 1. Conversely, the low- and high-membership functions demonstrated low

or negligible membership degrees. By utilizing fuzzy logic in AC synthesis, the process is not only optimized but also provided with a robust framework for decision making in uncertain situations. This method integrates expert knowledge and experimental data, resulting in more reliable and consistent results. Furthermore, the triangular membership function utilized in this study offers a straightforward yet efficient approach to model the relationship between the activation temperature and AC quality, rendering it particularly advantageous for industrial applications.

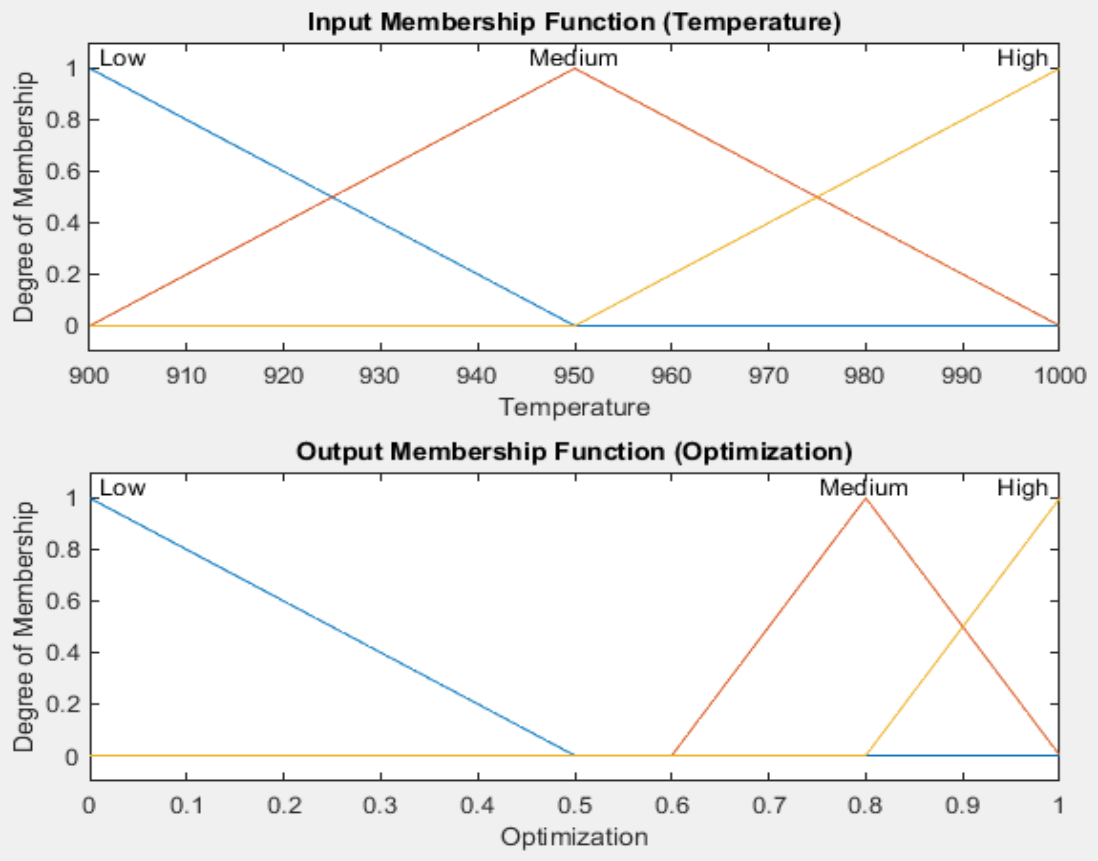

Figure 4. Fuzzy membership function: (a) Input (temperature), (b) Output (optimization)

3.2. Chemical analysis

AC was produced at an activation temperature of 950 °C. **Table 1** displays the results of the proximate analysis of the generated AC. The results revealed an AC yield of 26.29%, indicating that approximately one-quarter of the initial coconut shell material was successfully transformed into AC through the multi-stage synthesis process. Furthermore, the bulk density of the AC was measured at 0.519 g/ml, which represents the density of the final product. Ifa *et al.* (2021) suggested that AC derived from natural coconut components typically has a bulk density ranging from 0.31 to 0.52 g/ml [58]. This finding confirms the effectiveness of the synthesis method employed in this study, which uses fuzzy logic to control the production process.

Table 1. AC characteristics derived from CS with an activated temperature of 950 °C.

Yield (%)	Bulk density (g/ml)	Ash (%)	Moisture (%)	Volatile (%)	FCC (%)
26.29	0.52	4.33	7.21	16.32	72.14

The ash content of the AC produced in this study was determined to be 4.653%. This value substantiates the quantity of residues remaining after the combustion of the material. This ash content value was determined as part of the evaluation of the purity level of the obtained AC. The moisture content was

determined to be 12.348%. This finding indicates that the AC produced retains moisture content at this level. Finally, the volatile matter content indicates the presence of material components that are prone to buoyancy during combustion. The AC produced exhibited a volatile matter content of 39.863%. The evaluation of these values led to the conclusion that the FCC of the manufactured AC was 72.136%. This value is within the acceptable range stipulated by Ni'mah *et al.* (2024), who established that the FCC percentage of AC produced must fall within a minimum of 65% to be deemed successful, as referred to in SNI 06-3730-1995 [59].

3.2. XRD, FTIR and SEM-EDX Analysis

To support the proximate analysis results, XRD, FTIR, and SEM-EDX were conducted. XRD characterization revealed that the AC had an amorphous structure. The diffraction peaks observed at 2θ = 22° (**Figure 5)** further substantiate this finding. This assertion is further substantiated by the conclusions presented by Ahmad *et al.* (2022), who posited that AC possesses an amorphous structure, as substantiated by the peak at 2θ of approximately 22°. Additionally, a secondary pattern is identified in this graph at 2θ of approximately 30°, precisely at 34°. The observed peak was attributed to the characteristic diffraction pattern of calcite [60]. The finding of an amorphous structure is further corroborated by Prakash (2021), who revealed broad and sharp peaks in XRD characterization indicating an amorphous structure for AC [61].

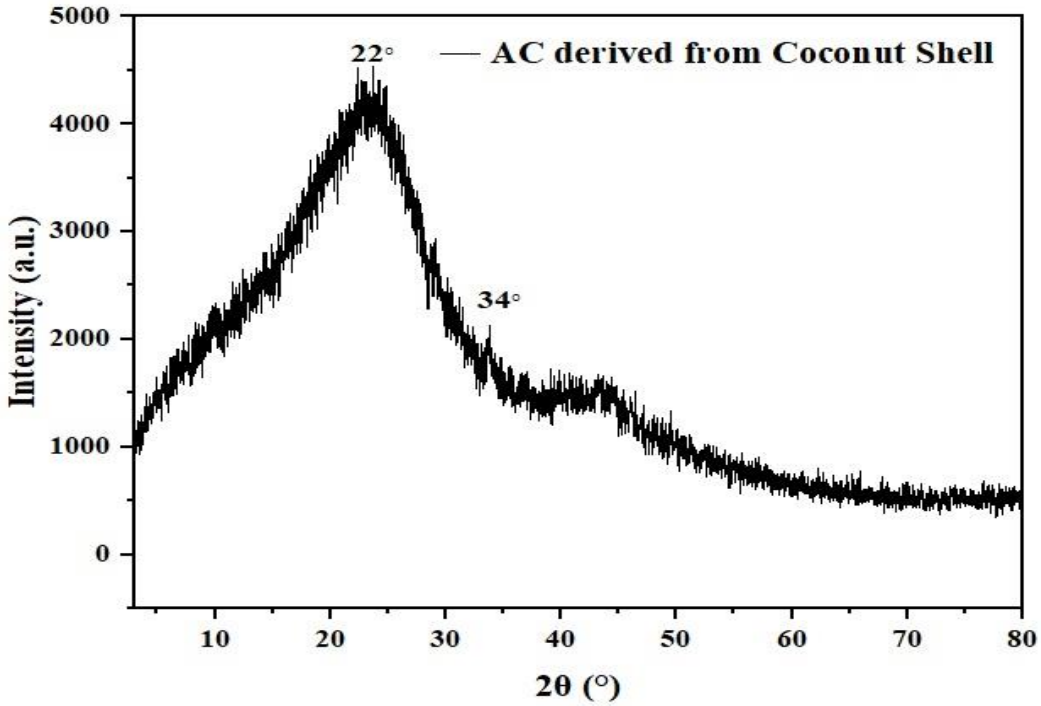

Figure 5. The XRD pattern of the AC derived from the coconut shell.

FTIR analysis was employed to assess the AC characteristics. The results of the FTIR characterization are illustrated in Figure 6, which presents the functional group patterns. FTIR spectra were recorded in the transmittance mode within the range of 500–4000 cm^{-1}. The predominant functional groups identified in AC include O-H, C-O, and C-H [62]. These functional groups are attributed to oxidation and reduction processes occurring during activation [63]. Ge *et al* [64] further demonstrated that each functional group corresponds to a specific wavelength region. For instance, the -OH stretching vibration appears at approximately 3000–3700 cm^{-1} [64], while the C–H stretching vibrations of alkanes, alkenes, and aromatics are observed within the range of 2800 – 3000 cm^{-1} [65]. The absorption peak around 1600 cm^{-1} is associated with N-H bending vibration [66], whereas the peak at 1380 cm^{-1} corresponds to the C–H bending vibration [67]. Additionally, the C–O stretching vibrations in ethers, esters, and phenols are detected within the range

of 1000–1300 cm^{-1} [68], and the C–H bending vibrations are observed between 650–1000 cm^{-1} [69].

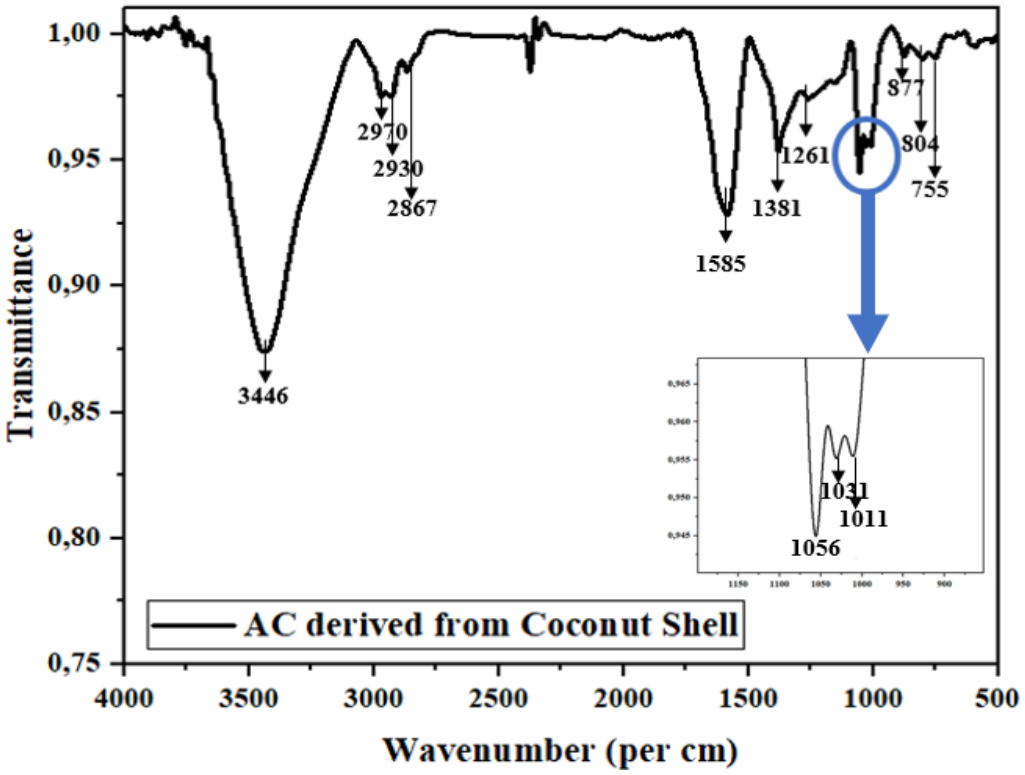

Figure 6. FTIR pattern of AC derived from coconut shell.

The functional groups identified in the FTIR patterns produced in this study are listed in Table 2. The identification of all the functional groups required by AC indicates successful synthesis in this study. Nevertheless, the presence of additional peaks indicates that the purity of the produced AC is compromised by impurities.

Table 2. Functional groups of AC produced from coconut shell by FTIR analysis.

Wavenumber (cm^{-1})	Type of vibration	Functional group	Ref.
3446	O-H stretching	Hydroxyl (Alcohols, Phenols)	[64]
2970	C-H stretching	Alkanes, Alkenes, Aromatics	[65]
2930	C-H stretching	Alkanes, Alkenes, Aromatics	[65]
2867	C-H stretching	Alkanes, Alkenes, Aromatics	[65]
1585	N-H bending	Amines, Amides	[66]
1381	C-H bending	Alkenes, Aromatics	[67]
1261	C-O stretching	Ethers, esters, and phenols	[68]
1056	C-O stretching	Ethers, esters, and phenols	[68]
1031	C-O stretching	Ethers, esters, and phenols	[68]
1011	C-O stretching	Ethers, esters, and phenols	[68]
877	C-H bending	Aromatics, Alkenes	[70]
804	C-H bending	Aromatics, Alkenes	[70]
755	C-H bending	Aromatics, Alkenes	[70]

In addition, SEM-EDX characterization was conducted to ascertain the morphological characteristics of the AC and the elemental content. The morphological structure of the synthesized AC is depicted in Figure 7, and the elemental content is summarized in Table 3. The figure shows that the morphological structure of the produced AC was uneven, with pores of different sizes. The identified pores confirmed the efficacy of the production process, as pores are the primary characteristic of AC. This observation is further

substantiated by the finding that the AC produced is exceptionally suitable for catalyst applications. According to Adeleye (2021), the presence of a substantial pore distribution in AC plays an important role in enhancing the effectiveness of the catalyst in absorbing vehicle exhaust pollutants [71]. EDX analysis showed that the carbon (C) content of the AC produced was approximately 72.4%, which was a good trend in the AC synthesis process. However, other materials were identified. These materials may be impurities.

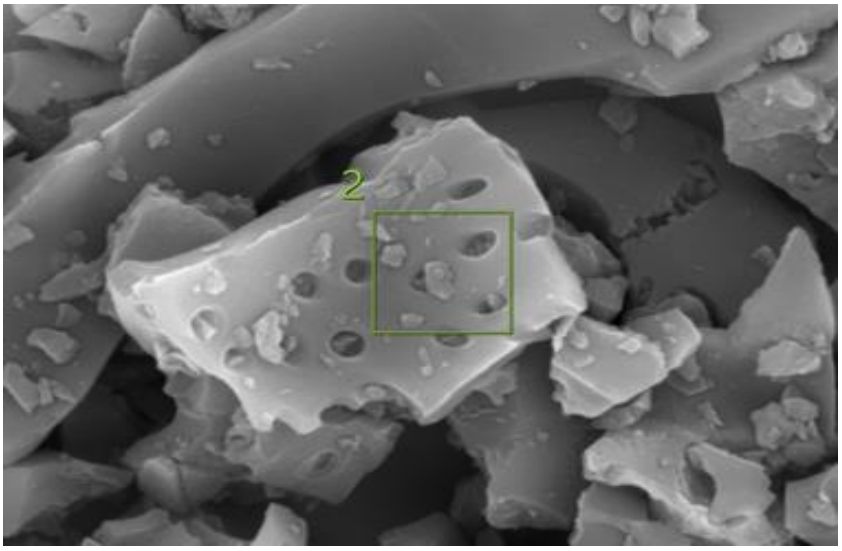

Figure 7. SEM of AC derived from coconut shells.

Table 3. Percentage of elements in AC with 950 °C activation temperature.

Characteristics	Element					
	C	O	Na	Si	K	Total
Weight (%)	72.4	8.8	0.9	17.7	0.2	100
Atomic (%)	83.1	7.6	0.5	8.7	0.1	100

3.3. Iodine number and vehicle performance

The iodine number test was used to evaluate the efficacy of the produced activated carbon (AC). This method, as highlighted by Cendekia *et al.* [72], assesses AC's adsorption capabilities of AC. The test results provide crucial information regarding the ability of the material to eliminate pollutants from water-based solutions. Several factors, such as surface area, pore size distribution, and surface chemistry, can affect AC's adsorption capacity of AC. Comprehending these aspects is essential for enhancing AC's performance of AC in water treatment and developing more efficient adsorbent materials.

This study utilized the iodine number test to measure AC's effectiveness of AC as a catalytic converter. The generated AC exhibited an iodine number of 613 mg/g, which is consistent with the medium standard for gas adsorption application. To showcase its gas absorption abilities, the AC was shaped into a doughnut-like catalytic converter and directly evaluated for its capacity to absorb exhaust gases, particularly CO and HC. The test results, illustrated in Figure 8, demonstrate a substantial reduction in CO exhaust emissions by approximately 86.04% and a significant decrease in HC emissions by approximately 56.79%. These findings suggest AC's potential of AC to reduce vehicle exhaust gas levels and its suitability for large-scale industrial production. Additionally, the results support the notion that fuzzy logic can effectively determine the optimal AC conditions.

Further testing was conducted to assess the impact of the AC as a catalytic converter on the vehicle engine performance. This study aimed to determine whether incorporating an AC-based catalytic converter would result in decreased engine performance.

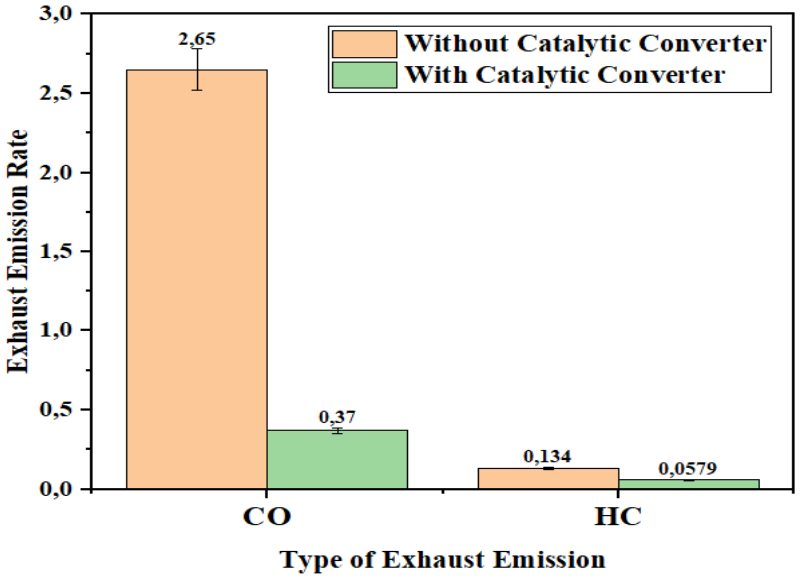

Figure 8. Comparison of exhaust emissions with and without a catalytic converter based on activated carbon.

A dynamometer was used to compare the power and torque values of the vehicle before and after integrating the AC-based catalytic converter. The results of this investigation are presented in Table 4.The test outcomes indicated that the catalytic converter led to a reduction in torque and power values. However, catalytic converters continue to have a positive impact on vehicle performance, particularly in mitigating exhaust emissions. The observed decrease in torque and power performance remained within acceptable limits, making this a viable option for everyday use.

Table 4. Vehicle performance testing through a dynamometer test.

Sample	Torque (Nm)	Power (HP)
Without catalytic converter	14.94	8.70
With catalytic converter	14.57	8.58

HP= horse power

4. Conclusions

This study demonstrated that fuzzy logic provides valuable insights into the optimization of AC synthesis, particularly in the context of temperature-based activation. Utilizing the triangle membership function, this fuzzy logic method demonstrated that 950 °C is the optimal activation temperature, leading to the realization of the most desirable properties in AC. Preliminary testing was conducted to investigate the characteristics of the AC based on the findings. The testing procedures entailed a series of proximate analyses, including the determination of ash content, moisture content, volatile matter, and FCC. The outcomes of these analyses were expressed as 4.332%, 7.211%, 16.321%, and 72.136%, respectively. Subsequently, the AC was subjected to iodine number testing, a method used to ascertain its adsorption performance. The iodine number was 613 mg/g, confirming the efficacy of the AC for gas adsorption. The effectiveness of the AC was demonstrated through its implementation as a catalytic converter, which was subjected to direct testing to determine its capacity to reduce CO and HC exhaust gases. The experimental findings revealed that the AC-based catalytic converter exhibited a significant reduction in CO and HC levels by 86.04% and 56.79%, respectively. To confirm the suitability of the catalytic converter for the vehicle, a series of dynamometer tests was performed. The ensuing test results exhibited a decline in torque and power values; however, these measurements remained within acceptable parameters for typical daily utilization. These findings are hypothesized to serve as a foundation for the large-scale production of AC-based catalytic converters in industrial settings.

AUTHOR'S DECLARATION

Authors' contributions and responsibilities

Diansyah Marbun: Conducted data collection and investigation and wrote the original draft of the manuscript. **Muhamad Taufik Ulhakim:** Contributed to writing, reviewing, and editing the original draft; supervised the study; developed the methodology and conceptualized the project; and conducted fuzzy logic modeling for result analysis. **Sukarman Sukarman:** Supervised the study, validated the results, and addressed reviewer comments. **Agus Supriyanto:** Provided supervision and contributed to the methodology and conceptualization of data collection procedures. **Ade Suhara**: Supervised the study and validated its results. **Auliya Rahmatul Ummah**: Contributed to the writing, reviewing, and editing of the original draft. **Neng Astri Lidiawati**: Contributed to writing, reviewing, and editing the original draft, and conducted fuzzy logic modeling for result analysis.

Acknowledgment

The authors acknowledge the comprehensive support provided by Universitas Buana Perjuangan Karawang through the Lembaga Penelitian dan Pengabdian Masyarakat (LPPM) for this project, as evidenced by project number 657/LPPM/ST/2024.

Availability of data and materials

All data are available from the corresponding author.

Competing interests

The authors declare no conflicts of interest.

REFERENCES

[1] P. Rajakrishnamoorthy *et al.*, "Exhaust emission control of SI engines using ZSM-5 zeolite supported bimetals as a catalyst synthesized from coal fly ash," *Fuel*, vol. 340, May 2023, doi: 10.1016/j.fuel.2022.127380.

[2] C. Leishman *et al.*, "Manganese-based catalysts supported on carbon xerogels for the selective catalytic reduction of NOx using a hollow fibre-based reactor," *Catal Today*, vol. 423, Nov. 2023, doi: 10.1016/j.cattod.2023.01.026.

[3] Q. Zhao, J. Li, A. Jiao, F. Liu, H. Xu, and X. Liao, "Pollutant emission characteristics of the close-coupled selective catalytic reduction system for diesel engines under low exhaust temperature conditions," *Fuel*, vol. 354, Dec. 2023, doi: 10.1016/j.fuel.2023.129303.

[4] D. Yang, Q. Yang, W. Ma, X. Ma, S. Wang, and Y. Lei, "Characteristics of spent automotive catalytic converters and their effects on recycling platinum-group-metals and rare-earth-elements," *Sep Purif Technol*, vol. 308, Mar. 2023, doi: 10.1016/j.seppur.2022.122977.

[5] A. Kozina, G. Radica, and S. Nižetić, "Analysis of methods towards reduction of harmful pollutants from diesel engines," *J Clean Prod*, vol. 262, Jul. 2020, doi: 10.1016/j.jclepro.2020.121105.

[6] S. Singha, M. I. Hossain, T. H. Toushi, and J. N. Nimu, "Catalytic Converter and Its Revolution for Automobile Exhaust Emissions: A Review," 2022.

[7] B. Zhang, X. Li, Q. Wan, B. Liu, G. Jia, and Z. Yin, "Hydrocarbon emission control of an adsorptive catalytic gasoline particulate filter during cold-start period of the gasoline engine," *Energy*, vol. 262, Jan. 2023, doi: 10.1016/j.energy.2022.125445.

[8] D. J. Deka, J. A. Pihl, C. R. Thomas, and W. P. Partridge, "Intra-catalyst CH4 oxidation pathways on a Pd/Al2O3/CeZrOx-based commercial catalyst and implications on NOx conversion profiles for a natural gas vehicle exhaust under lambda modulation," *Chemical Engineering Journal*, vol. 472, Sep. 2023, doi: 10.1016/j.cej.2023.144803.

[9] P. N. R. Vennestrøm, J. R. Thøgersen, P. L. T. Gabrielsson, L. Van Tendeloo, F. W. Schütze, and M. Moliner, "Advances and perspectives from a decade of collaborative efforts on zeolites for

selective catalytic reduction of NOx," *Microporous and Mesoporous Materials*, vol. 358, Aug. 2023, doi: 10.1016/j.micromeso.2022.112336.

[10] Z. Zhang *et al.*, "Multi-objective optimization of the three-way catalytic converter on the combustion and emission characteristics for a gasoline engine," *Energy*, vol. 277, Aug. 2023, doi: 10.1016/j.energy.2023.127634.

[11] L. Sun *et al.*, "Double-stable Ce-based oxide: Capturing atomic precious metals via Ostwald ripening for multicomponent three-way catalysts construction," *Molecular Catalysis*, vol. 554, Feb. 2024, doi: 10.1016/j.mcat.2023.113808.

[12] G. Brinklow *et al.*, "Non-carbon greenhouse gas emissions for hybrid electric vehicles: three-way catalyst nitrous oxide and ammonia trade-off," *International Journal of Environmental Science and Technology*, vol. 20, no. 11, pp. 12521–12532, Nov. 2023, doi: 10.1007/s13762-023-04848-2.

[13] S. Sharma Gunasekaran, S. Manivannan, and P. Ramakrishnan, "An experimental investigation on regulated and unregulated emissions of a gasohol fueled SI engine with a novel three way catalytic converter," *Journal Europeen des Systemes Automatises*, vol. 53, no. 2, pp. 219–224, Apr. 2020, doi: 10.18280/jesa.530208.

[14] N. Udhayakumar, S. Ramesh Babu, R. Bharathwaaj, and R. Sathyamurthy, "An experimental study on emission characteristics in compression ignition engine with silver and zinc coated catalytic converter," in *Materials Today: Proceedings*, Elsevier Ltd, 2021, pp. 4959–4964. doi: 10.1016/j.matpr.2021.04.314.

[15] C. Özyalcin, S. Sterlepper, S. Roiser, H. Eichlseder, and S. Pischinger, "Exhaust gas aftertreatment to minimize NOX emissions from hydrogen-fueled internal combustion engines," *Appl Energy*, vol. 353, Jan. 2024, doi: 10.1016/j.apenergy.2023.122045.

[16] A. M. Moschovi *et al.*, "First of its kind automotive catalyst prepared by recycled pgms-catalytic performance," *Catalysts*, vol. 11, no. 8, Aug. 2021, doi: 10.3390/catal11080942.

[17] R. S. Kumar and S. S. Kumaran, "NOx, CO & HC control by adopting activated charcoal enriched filter in catalytic converter of diesel engine," *Mater Today Proc*, vol. 22, pp. 2283–2290, 2020, [Online]. Available: www.sciencedirect.com

[18] T. K. Kurse, R. B. Nallamothu, and M. Liben, "Reduction of Harmful Emissions from IC Engines using Hybrid Aqua Charcoal Replacing both Silencer and Catalytic Converter," *Journal of Offshore Structure and Technology*, vol. 7, no. 3, pp. 1–5, 2020, [Online]. Available: www.stmjournals.com

[19] J. Akinbomi, Salami, and Moshood, "Generator Exhausts Control in Nigeria using Activated Carbon from Discarded Rubber Tyres," *International Journal of Engineering Research and Technology (IJERT)*, vol. 11, no. 02, pp. 100–107, 2022, [Online]. Available: www.ijert.org

[20] A. Hamid *et al.*, "An Improvement of Catalytic Converter Activity Using Copper Coated Activated Carbon Derived from Banana Peel," *International Journal of Renewable Energy Development*, vol. 12, no. 1, pp. 144–154, Jan. 2023, doi: 10.14710/ijred.2023.48739.

[21] Ya' Muhammad Arsyad *et al.*, "Effect of TiO2 on Orange Peel Activated Carbon Composite in Reducing Carbon Monoxide and Hydrocarbon Gas Emissions," *Jurnal Ilmu Fisika*, vol. 15, no. 2, pp. 73–80, Apr. 2023, doi: 10.25077/jif.15.2.73-80.2023.

[22] A. S. Elkholy, M. S. Yahia, M. A. Elnwawy, H. A. Gomaa, and A. S. Elzaref, "Synthesis of activated carbon composited with Egyptian black sand for enhanced adsorption performance toward methylene blue dye," *Sci Rep*, vol. 13, no. 1, Dec. 2023, doi: 10.1038/s41598-023-28556-6.

[23] A. Hamid *et al.*, "Pemanfaatan Karbon Aktif dari Limbah Kulit Pisang untuk Catalytic Converter pada Mesin Diesel," *Jurnal Rekayasa Mesin*, vol. 12, no. 3, pp. 709–716, Dec. 2021, doi: 10.21776/ub.jrm.2021.012.03.20.

[24] D. Ahmad Fajri, A. Ghofur, and P. Studi Teknik Mesin, "Pengaruh Arang Kayu Ulin Sebagai Catalytic Converter Terhadap Emisi Gas Buang dan Konsumsi Bahan Bakar Pada Mesin Toyota

Kijang 5K," *JTAM Rotary*, vol. 3, no. 2, 2021, [Online]. Available: https://ppjp.ulm.ac.id/journals/index.php/rot

[25] A. Sulton and A. Ghofur, "Pengaruh Penggunaan Catalytic Converter Berbahan Arang Kayu Alaban Dengan Aditif Tembaga (Cu) Terhadap Emisi Gas Buang Dan Konsumsi Bahan Bakar Pada Toyota Kijang 5K," *JTAM Rotary*, vol. 3, no. 1, 2021, [Online]. Available: https://ppjp.ulm.ac.id/journals/index.php/rot

[26] H. K. Yağmur and İ. Kaya, "Synthesis and characterization of magnetic ZnCl2-activated carbon produced from coconut shell for the adsorption of methylene blue," *J Mol Struct*, vol. 1232, May 2021, doi: 10.1016/j.molstruc.2021.130071.

[27] S. Wang *et al.*, "Halloysite and coconut shell biochar magnetic composites for the sorption of Pb(II) in wastewater: Synthesis, characterization and mechanism investigation," *J Environ Chem Eng*, vol. 9, no. 6, Dec. 2021, doi: 10.1016/j.jece.2021.106865.

[28] T. R. Brazil, M. Gonçalves, M. S. O. Junior, and M. C. Rezende, "A statistical approach to optimize the activated carbon production from Kraft lignin based on conventional and microwave processes," *Microporous and Mesoporous Materials*, vol. 308, Dec. 2020, doi: 10.1016/j.micromeso.2020.110485.

[29] W. Spencer, G. Senanayake, M. Altarawneh, D. Ibana, and A. N. Nikoloski, "Review of the effects of coal properties and activation parameters on activated carbon production and quality," Jul. 15, 2024, *Elsevier Ltd*. doi: 10.1016/j.mineng.2024.108712.

[30] M. Gayathiri, T. Pulingam, K. T. Lee, and K. Sudesh, "Activated carbon from biomass waste precursors: Factors affecting production and adsorption mechanism," May 01, 2022, *Elsevier Ltd*. doi: 10.1016/j.chemosphere.2022.133764.

[31] A. Chakraborty, A. Pal, and B. B. Saha, "A Critical Review of the Removal of Radionuclides from Wastewater Employing Activated Carbon as an Adsorbent," Dec. 01, 2022, *MDPI*. doi: 10.3390/ma15248818.

[32] G. Rajkumar *et al.*, "Parametric Optimization of Powder-Mixed EDM of AA2014/Si3N4/Mg/Cenosphere Hybrid Composites Using Fuzzy Logic: Analysis of Mechanical, Machining, Microstructural, and Morphological Characterizations," *Journal of Composites Science*, vol. 7, no. 9, Sep. 2023, doi: 10.3390/jcs7090380.

[33] Y. Wang, Z. Wang, and G. G. Wang, "Hierarchical learning particle swarm optimization using fuzzy logic," *Expert Syst Appl*, vol. 232, Dec. 2023, doi: 10.1016/j.eswa.2023.120759.

[34] H. Javadian, M. Ghasemi, M. Ruiz, A. M. Sastre, S. M. H. Asl, and M. Masomi, "Fuzzy logic modeling of Pb (II) sorption onto mesoporous NiO/ZnCl2-Rosa Canina-L seeds activated carbon nanocomposite prepared by ultrasound-assisted co-precipitation technique," *Ultrason Sonochem*, vol. 40, pp. 748–762, Jan. 2018, doi: 10.1016/j.ultsonch.2017.08.022.

[35] Mohammad Ghassan Alghifari *et al.*, "Implementation and Comparison of Coffee Bean Drying Temperature SettingsBased on Fuzzy Logic," *Journal of Applied Science, Technology & Humanities*, vol. 1, no. 5, pp. 493–507, Nov. 2024, doi: 10.62535/cj817x36.

[36] O. Ofe, A. Ajayi, U. Bagaye, and E. AGBON, "Empirical Investigative Analysis on the Effect of Triangular and Gaussian Membership Function on Fuzzy-based Controlled Vehicle Platooning," *Nigerian Journal of Engineering*, vol. 30, no. 3, p. 28, 2023, doi: 10.5455/nje.2023.30.03.05.

[37] F. C. Jong and M. M. Ahmed, "Novel GIS-based fuzzy TOPSIS and filtration algorithms for extra-large scale optimal solar energy sites identification," *Solar Energy*, vol. 268, Jan. 2024, doi: 10.1016/j.solener.2023.112274.

[38] E. Natarajan, F. Augustin, M. K. A. Kaabar, C. R. Kenneth, and K. Yenoke, "Various defuzzification and ranking techniques for the heptagonal fuzzy number to prioritize the vulnerable countries of stroke disease," *Results in Control and Optimization*, vol. 12, Sep. 2023, doi:

10.1016/j.rico.2023.100248.

[39] S. J. Rajasekaran and V. Raghavan, "Facile synthesis of activated carbon derived from Eucalyptus globulus seed as efficient electrode material for supercapacitors," *Diam Relat Mater*, vol. 109, Nov. 2020, doi: 10.1016/j.diamond.2020.108038.

[40] X. L. Tian, J. H. Yu, L. Qiu, Y. H. Zhu, and M. Q. Zhu, "Structural changes and electrochemical properties of mesoporous activated carbon derived from Eucommia ulmoides wood tar by KOH activation for supercapacitor applications," *Ind Crops Prod*, vol. 197, Jul. 2023, doi: 10.1016/j.indcrop.2023.116628.

[41] E. H. Sujiono *et al.*, "Fabrication and characterization of coconut shell activated carbon using variation chemical activation for wastewater treatment application," *Results Chem*, vol. 4, Jan. 2022, doi: 10.1016/j.rechem.2022.100291.

[42] S. Z. Naji and C. T. Tye, "A review of the synthesis of activated carbon for biodiesel production: Precursor, preparation, and modification," *Energy Conversion and Management: X*, vol. 13, Jan. 2022, doi: 10.1016/j.ecmx.2021.100152.

[43] W. S. Muleta, S. M. Denboba, and A. B. Bayu, "Corncob-supported calcium oxide nanoparticles from hen eggshells for cadmium (Cd-II) removal from aqueous solutions; Synthesis and characterization," *Heliyon*, vol. 10, no. 6, Mar. 2024, doi: 10.1016/j.heliyon.2024.e27767.

[44] I. Neme, G. Gonfa, and C. Masi, "Preparation and characterization of activated carbon from castor seed hull by chemical activation with H3PO4," *Results in Materials*, vol. 15, Sep. 2022, doi: 10.1016/j.rinma.2022.100304.

[45] N. Bouchelkia *et al.*, "Jujube stones based highly efficient activated carbon for methylene blue adsorption: Kinetics and isotherms modeling, thermodynamics and mechanism study, optimization via response surface methodology and machine learning approaches," *Process Safety and Environmental Protection*, vol. 170, pp. 513–535, Feb. 2023, doi: 10.1016/j.psep.2022.12.028.

[46] N. R. Ca Ndido, M. J. Prauchner, A. D. O. Vilela, and V. N. M. D. Pasa, "The use of gases generated from eucalyptus carbonization as activating agent to produce activated carbon: An integrated process," *J Environ Chem Eng*, vol. 8, no. 4, Aug. 2020, doi: 10.1016/j.jece.2020.103925.

[47] D. Dimbo *et al.*, "Methylene blue adsorption from aqueous solution using activated carbon of spathodea campanulata," *Results in Engineering*, vol. 21, Mar. 2024, doi: 10.1016/j.rineng.2024.101910.

[48] A. Ibrahim *et al.*, "Preparation and characterization of activated carbon obtained from Melaleuca cajuputi leaves," *Carbon Trends*, vol. 13, Dec. 2023, doi: 10.1016/j.cartre.2023.100301.

[49] T. C. Egbosiuba *et al.*, "Ultrasonic enhanced adsorption of methylene blue onto the optimized surface area of activated carbon: Adsorption isotherm, kinetics and thermodynamics," *Chemical Engineering Research and Design*, vol. 153, pp. 315–336, Jan. 2020, doi: 10.1016/j.cherd.2019.10.016.

[50] J. Fito, S. Tibebu, and T. T. I. Nkambule, "Optimization of Cr (VI) removal from aqueous solution with activated carbon derived from Eichhornia crassipes under response surface methodology," *BMC Chem*, vol. 17, no. 1, Dec. 2023, doi: 10.1186/s13065-023-00913-6.

[51] E. R. Raut, M. A. Bedmohata, and A. R. Chaudhari, "Comparative study of preparation and characterization of activated carbon obtained from sugarcane bagasse and rice husk by using H3PO4 and ZnCl2," in *Materials Today: Proceedings*, Elsevier Ltd, Jan. 2022, pp. 1875–1884. doi: 10.1016/j.matpr.2022.05.413.

[52] W. Spencer, D. Ibana, P. Singh, and A. N. Nikoloski, "Effect of Surface Area, Particle Size and Acid Washing on the Quality of Activated Carbon Derived from Lower Rank Coal by KOH Activation," *Sustainability*, vol. 16, no. 14, p. 5876, Jul. 2024, doi: 10.3390/su16145876.

[53] S. Shabir, S. Z. Hussain, T. A. Bhat, T. Amin, M. Beigh, and S. Nabi, "High Carbon content

Microporous Activated Carbon from Thin Walnut Shells: Optimization, Physico-Chemical Analysis and Structural Profiling"," *Process Safety and Environmental Protection*, Jun. 2024, doi: 10.1016/j.psep.2024.06.121.

[54] X. Li, L. Zhang, Z. Yang, P. Wang, Y. Yan, and J. Ran, "Adsorption materials for volatile organic compounds (VOCs) and the key factors for VOCs adsorption process: A review," *Sep Purif Technol*, vol. 235, Mar. 2020, doi: 10.1016/j.seppur.2019.116213.

[55] M. Şirazi and S. Aslan, "Comprehensive characterization of high surface area activated carbon prepared from olive pomace by KOH activation," *Chem Eng Commun*, vol. 208, no. 10, pp. 1479–1493, 2021, doi: 10.1080/00986445.2020.1864628.

[56] S. Dey and G. Chandra Dhal, "Controlling carbon monoxide emissions from automobile vehicle exhaust using copper oxide catalysts in a catalytic converter," Sep. 01, 2020, *Elsevier Ltd*. doi: 10.1016/j.mtchem.2020.100282.

[57] X. Liang *et al.*, "Polyvinyl Alcohol (PVA)-Based Hydrogels: Recent Progress in Fabrication, Properties, and Multifunctional Applications," Oct. 01, 2024, *Multidisciplinary Digital Publishing Institute (MDPI)*. doi: 10.3390/polym16192755.

[58] L. Ifa, N. Nurjannah, T. Syarif, and D. Darnengsih, *Bioadsorben dan Aplikasinya*. Yayasan Pendidikan Cendekia Muslim, 2021. [Online]. Available: https://www.researchgate.net/publication/357393346

[59] L. Ni`mah *et al.*, "Karakteristik Karbon Aktif Teraktifasi Hɜpo4 dari Limbah Sereh (Cymbopogon S.P)," *Journal of Chemical Process Engineering*, vol. 9, no. 1, pp. 60–69, May 2024, doi: 10.33096/jcpe.v9i1.686.

[60] R. Kabir Ahmad, S. Anwar Sulaiman, S. Yusup, S. Sham Dol, M. Inayat, and H. Aminu Umar, "Exploring the potential of coconut shell biomass for charcoal production," *Ain Shams Engineering Journal*, vol. 13, no. 1, Jan. 2022, doi: 10.1016/j.asej.2021.05.013.

[61] M. Om Prakash, G. Raghavendra, S. Ojha, and M. Panchal, "Characterization of porous activated carbon prepared from arhar stalks by single step chemical activation method," in *Materials Today: Proceedings*, Elsevier Ltd, 2020, pp. 1476–1481. doi: 10.1016/j.matpr.2020.05.370.

[62] J. Long, P. He, K. Przystupa, Y. Wang, and O. Kochan, "Preparation of Oily Sludge-Derived Activated Carbon and Its Adsorption Performance for Tetracycline Hydrochloride," *Molecules*, vol. 29, no. 4, Feb. 2024, doi: 10.3390/molecules29040769.

[63] D. R. Lobato-Peralta *et al.*, "Advances in activated carbon modification, surface heteroatom configuration, reactor strategies, and regeneration methods for enhanced wastewater treatment," *J Environ Chem Eng*, vol. 9, no. 4, Aug. 2021, doi: 10.1016/j.jece.2021.105626.

[64] L. Ge *et al.*, "An analysis of the carbonization process of coal-based activated carbon at different heating rates," *Energy*, vol. 267, Mar. 2023, doi: 10.1016/j.energy.2022.126557.

[65] H. A. Baloch *et al.*, "Catalytic upgradation of bio-oil over metal supported activated carbon catalysts in sub-supercritical ethanol," *J Environ Chem Eng*, vol. 9, no. 2, Apr. 2021, doi: 10.1016/j.jece.2021.105059.

[66] A. Rana and T. A. Saleh, "An investigation of polymer-modified activated carbon as a potential shale inhibitor for water-based drilling muds," *J Pet Sci Eng*, vol. 216, Sep. 2022, doi: 10.1016/j.petrol.2022.110763.

[67] B. Shoukat *et al.*, "Microwaves assisted deconstruction of HDPE waste into structured carbon and hydrogen fuel using Al2O3-(Ni, Zn, Mg)Fe2O4 composite catalysts," *Thermal Science and Engineering Progress*, vol. 47, Jan. 2024, doi: 10.1016/j.tsep.2023.102368.

[68] S. M. Waly, A. M. El-Wakil, W. M. A. El-Maaty, and F. S. Awad, "Efficient removal of Pb(II) and Hg(II) ions from aqueous solution by amine and thiol modified activated carbon," *Journal of Saudi Chemical Society*, vol. 25, no. 8, Aug. 2021, doi: 10.1016/j.jscs.2021.101296.

[69] H. Nath, J. Das, C. Debnath, B. Sarkar, R. Saxena, and S. D. Barma, "Development of lignocellulosic biomass derived Cu and Zn doped highly porous activated carbon and its utilization in the anti-microbial treatment," *Environmental Chemistry and Ecotoxicology*, vol. 5, pp. 155–164, Jan. 2023, doi: 10.1016/j.enceco.2023.07.001.

[70] H. Nath, J. Das, C. Debnath, B. Sarkar, R. Saxena, and S. D. Barma, "Development of lignocellulosic biomass derived Cu and Zn doped highly porous activated carbon and its utilization in the anti-microbial treatment," *Environmental Chemistry and Ecotoxicology*, vol. 5, pp. 155–164, Jan. 2023, doi: 10.1016/j.enceco.2023.07.001.

[71] A. T. Adeleye *et al.*, "Efficient synthesis of bio-based activated carbon (AC) for catalytic systems: A green and sustainable approach," Apr. 25, 2021, *Korean Society of Industrial Engineering Chemistry*. doi: 10.1016/j.jiec.2021.01.044.

[72] D. Cendekia, D. Ayu Afifah, and W. Hanifah, "Linearity Graph in the Prediction of Granular Active Carbon (GAC) Adsorption Ability," in *IOP Conference Series: Earth and Environmental Science*, IOP Publishing Ltd, Apr. 2021. doi: 10.1088/1755-1315/1012/1/012079.